Article

Cell Reports

Lack of Transcription Triggers H3K27me3 Accumulation in the Gene Body

Graphical Abstract

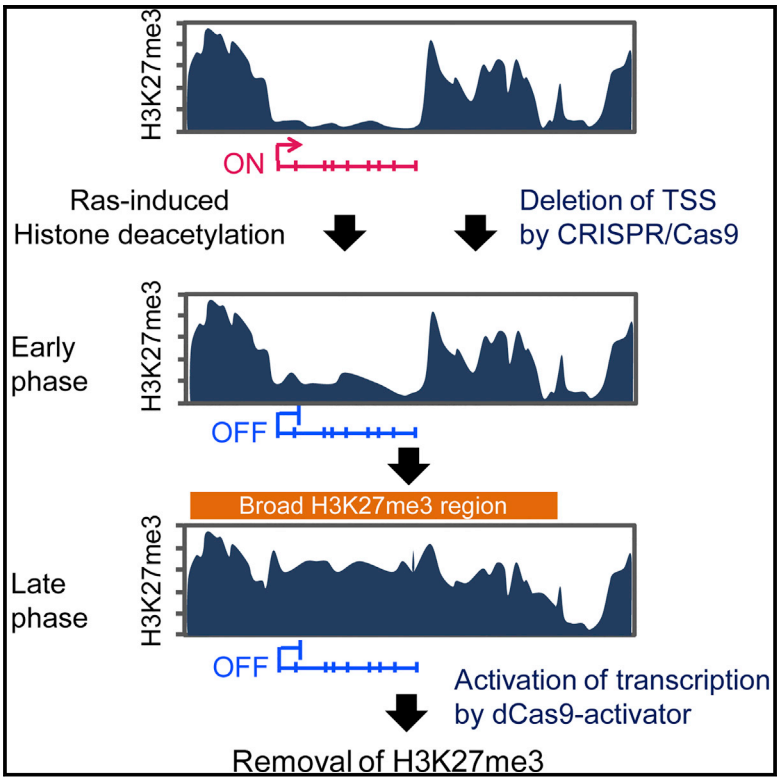

Highlights

- Deletion of the transcription start site increases H3K27me3 level in the gene body
- Histone deacetylation mediates Ras-induced gene silencing and the H3K27me3 increase
- Maximal Ras-induced accumulation of H3K27me3 requires at least 35 days
- Ras-induced H3K27me3 accumulation is reversed by forced activation of transcription

Authors

Masaki Hosogane, Ryo Funayama, Matsuyuki Shirota, Keiko Nakayama

Correspondence

nakayak2@med.tohoku.ac.jp

In Brief

Hosogane et al. demonstrate that changes in transcriptional activity regulate H3K27me3 histone modification. Direct abrogation of transcription induced by deletion of the transcription start site is sufficient to trigger accumulation of H3K27me3. Conversely, forced activation of transcription is sufficient to remove H3K27me3 deposited in response to oncogenic Ras signaling.

Hosogane et al., 2016, Cell Reports *16*, 696–706
July 19, 2016
http://dx.doi.org/10.1016/j.celrep.2016.06.034

OPEN ACCESS
CellPress

Cell Reports
Article

Lack of Transcription Triggers H3K27me3 Accumulation in the Gene Body

Masaki Hosogane,[1] Ryo Funayama,[1] Matsuyuki Shirota,[2] and Keiko Nakayama[1,*]
[1]Department of Cell Proliferation, United Center for Advanced Research and Translational Medicine, Graduate School of Medicine, Tohoku University, 2-1 Seiryo-machi, Aoba-ku, Sendai 980-8575, Japan
[2]Division of Interdisciplinary Medical Sciences, United Center for Advanced Research and Translational Medicine, Graduate School of Medicine, Tohoku University, 2-1 Seiryo-machi, Aoba-ku, Sendai 980-8575, Japan
*Correspondence: nakayak2@med.tohoku.ac.jp
http://dx.doi.org/10.1016/j.celrep.2016.06.034

SUMMARY

Trimethylated H3K27 (H3K27me3) is associated with transcriptional repression, and its abundance in chromatin is frequently altered in cancer. However, it has remained unclear how genomic regions modified by H3K27me3 are specified and formed. We previously showed that downregulation of transcription by oncogenic Ras signaling precedes upregulation of H3K27me3 level. Here, we show that lack of transcription as a result of deletion of the transcription start site of a gene is sufficient to increase H3K27me3 content in the gene body. We further found that histone deacetylation mediates Ras-induced gene silencing and subsequent H3K27me3 accumulation. The H3K27me3 level increased gradually after Ras activation, requiring at least 35 days to achieve saturation. Such maximal accumulation of H3K27me3 was reversed by forced induction of transcription with the dCas9-activator system. Thus, our results indicate that changes in H3K27me3 level, especially in the body of a subset of genes, are triggered by changes in transcriptional activity itself.

INTRODUCTION

The elaborate control of histone modification is essential for various eukaryotic cellular functions including transcriptional regulation. Trimethylation at lysine-27 of histone H3 (H3K27) is mediated by Polycomb repressive complex 2 (PRC2) and associated with transcriptional repression (Di Croce and Helin, 2013; Simon and Kingston, 2013). The distribution of trimethylated H3K27 (H3K27me3) throughout the genome has been determined by genome-wide comprehensive analyses, such as those based on deep chromatin immunoprecipitation sequencing (ChIP-seq) (Dunham et al., 2012; Ernst et al., 2011). Such analyses have revealed an inverse relation between H3K27me3 level and transcriptional activity for various subsets of genes, including those encoding Hox proteins, cell-cycle regulators, and transcription factors. Although these observations have suggested that H3K27me3 plays a key role in transcriptional repression, they have not revealed the hierarchical order among recruitment of PRC2, deposition of H3K27me3, and transcriptional repression. Thus, it has remained unclear how genomic regions covered with H3K27me3 are specified and formed.

Studies in *Drosophila* have identified Polycomb response elements (PREs) to which PRC2 is recruited by specific DNA-binding proteins, such as PHO (Schwartz and Pirrotta, 2007). PRC2 is required for maintenance of the repressed state of genes whose expression has already been attenuated by repressive transcriptional factors, including segmentation gene products. On the other hand, establishment of gene silencing by PRC2 at PREs is prevented by the Trithorax complex, which mediates the trimethylation of H3K4 and transcriptional activation (Poux et al., 2002). These observations suggest that transcriptional activity itself plays a role in the regulation of PRC2 at PREs. However, it remains controversial whether transcription through PREs impedes the access of PRC2 (Erokhin et al., 2015; Schmitt et al., 2005). Furthermore, differences in PRC2 function and regulation have been detected among species, and definitive PREs corresponding to those in *Drosophila* have not been identified in mammalian cells to date (Bauer et al., 2016).

Recent studies with mammalian cells have shown that CpG islands have the potential to be targeted by PRC2 (Mendenhall et al., 2010) and that PRC2 is recruited to specific regions of DNA by several mechanisms mediated by noncoding RNA (da Rocha et al., 2014; Sarma et al., 2014), transcription factors (Dietrich et al., 2012), or PRC1-dependent ubiquitylation of histone H2A (Blackledge et al., 2014; Kalb et al., 2014). On the other hand, the possibility of regulation of PRC2 recruitment by transcription has been suggested by several observations, including the finding that prevention of RNA polymerase II function with chemical inhibitors increased H3K27me3 abundance at CpG islands in embryonic stem cells (ESCs) (Riising et al., 2014). Moreover, H3K27me3 deposition in the gene body was found to be induced when transcription was prematurely interrupted by insertion of polyadenylation site in ESCs (Kaneko et al., 2014). These various observations suggest that recruitment or activation of PRC2 follows transcriptional repression. At least two mechanisms of H3K27me3 deposition in mammals have therefore been proposed: active recruitment of PRC2 by specific binding partners and passive recruitment of PRC2 after transcriptional repression (Blackledge et al., 2015).

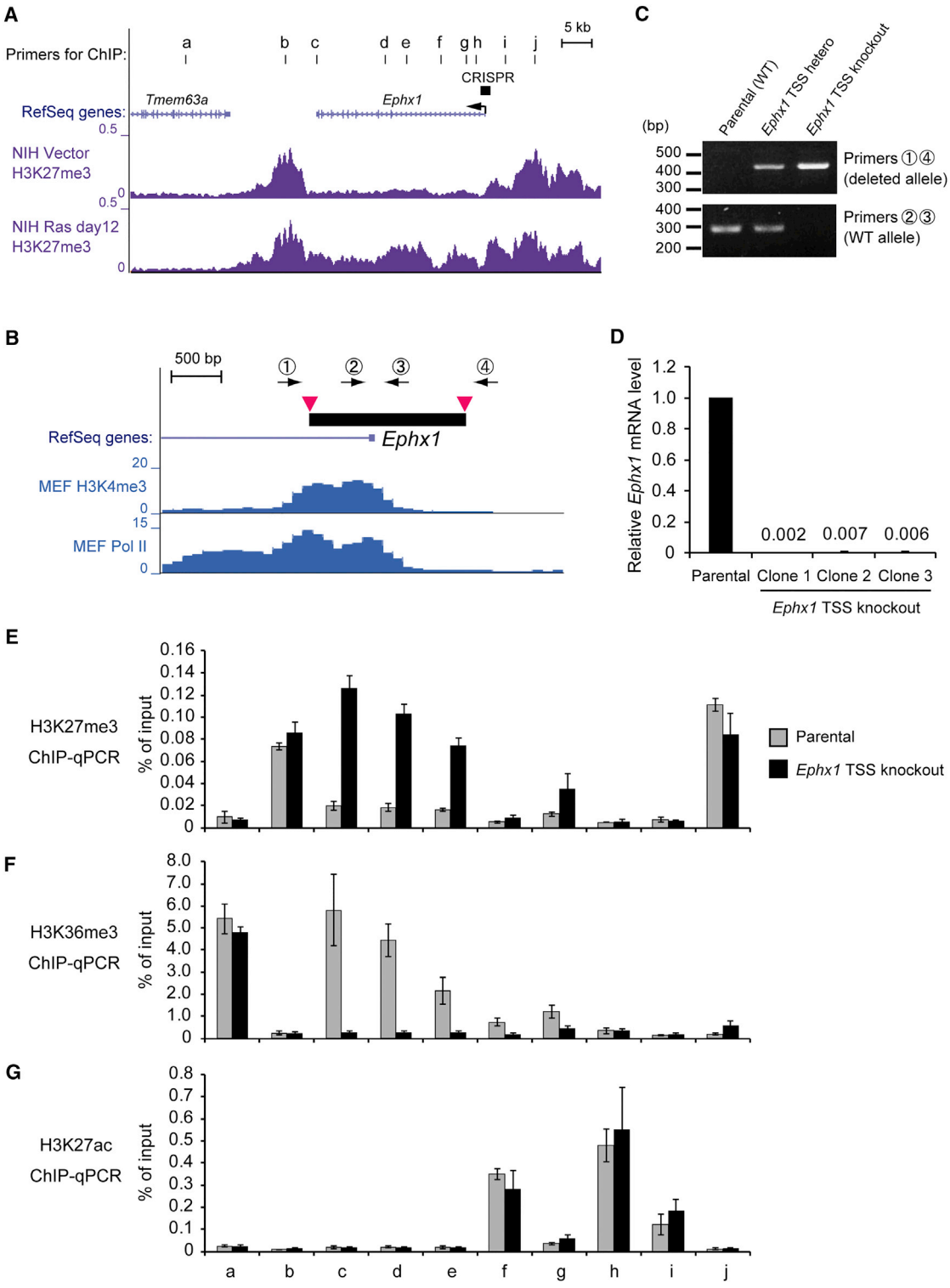

Figure 1. Lack of Transcription Is Sufficient to Induce Accumulation of H3K27me3 in the Gene Body of *Ephx1*

(A) H3K27me3 level at the *Ephx1* locus as revealed by our previous ChIP-seq analysis of control NIH 3T3 cells (NIH Vector) and cells at 12 days after the onset of H-Ras (G12V) (RasG12V) expression conferred by retroviral infection (NIH Ras day12). The positions of ChIP-qPCR primers are indicated by the lowercase letters (a–j). The black bar indicates the region targeted by the CRISPR/Cas9 genome editing system. Reads per million (RPMs) are used for the y axis in each track.

(legend continued on next page)

Lack or mutation of PRC2 components results in developmental defects during embryogenesis or in tumorigenesis, indicating the physiological relevance of H3K27me3 (Kim and Roberts, 2016; Surface et al., 2010). Furthermore, various environmental and developmental signals are known to regulate H3K27me3 levels dynamically. The small GTPase Ras transmits signals triggered by growth factor stimulation to downstream-signaling pathways, including those mediated by mitogen-activated protein kinases (MAPKs) (Karnoub and Weinberg, 2008). Activating mutations of Ras are one of the most frequent types of oncogenic mutation in human cancer. We have shown previously that oncogenic Ras signaling represses transcription of a subset of genes in association with a gradual increase in H3K27me3 level in cultured cells (Hosogane et al., 2013). Although our results indicated that transcriptional repression precedes upregulation of H3K27me3 in this experimental model of abnormal epigenetic modification in cancer, it has remained unclear whether physiological changes in H3K27me3 level induced by Ras signaling are a cause or consequence of changes in transcription.

We have now further examined the causal nature of the relation between H3K27 trimethylation and transcriptional silencing in response to activation of Ras signaling. With the use of the CRISPR/Cas9 system for genome editing to manipulate the state of transcription directly, we obtained evidence showing that transcription itself regulates H3K27me3 status and that the Ras-induced changes in H3K27me3 level are not completed until at least 30 days after those in transcription.

RESULTS

Lack of Transcription, but Not Ras Signaling, Is Sufficient to Induce H3K27 Trimethylation

Ephx1 is silenced by activation of Ras-MAPK signaling in NIH 3T3 mouse fibroblasts (Figure S1), and this silencing is accompanied by marked enrichment of H3K27me3 in the gene body (Figure 1A). We first examined whether Ras signaling or lack of transcription itself induces the change in H3K27me3 level of *Ephx1*. To silence gene expression without activating Ras signaling, we deleted a genomic region containing the transcription start site (TSS) of *Ephx1* with the use of CRISPR/Cas9-mediated genome engineering in NIH 3T3 cells (Ran et al., 2013; Zheng et al., 2014). We therefore designed two single-guide RNAs (sgRNAs) that target a 1.5-kb genomic region around the annotated TSS of *Ephx1* (Figure 1B). This region includes most of the H3K4me3 and RNA polymerase II peaks, which are indicative of the promoter region, as revealed by a public ChIP-seq database for mouse embryonic fibroblasts (MEFs). We transfected NIH 3T3 cells with plasmids encoding *Streptococcus pyogenes* Cas9 (SpCas9) and the two sgRNAs, and then we cloned the transfected cells for establishment of several *Ephx1* TSS-deleted cell lines. Deletion of the TSS of *Ephx1* was confirmed by genomic PCR analysis (Figure 1C).

As expected, transcription of *Ephx1* was abolished in the *Ephx1* TSS-deleted cells (Figure 1D). ChIP and qPCR analysis revealed that the amount of H3K27me3 in the gene body of *Ephx1* was markedly increased in these cells (Figure 1E). In contrast, H3K27me3 levels in genomic regions external to *Ephx1* were similar in the *Ephx1* TSS-deleted cells and parental cells, indicating that H3K27me3 was upregulated only in the gene body of *Ephx1*. Furthermore, consistent with the loss of *Ephx1* mRNA (Figure 1D), the abundance of H3K36me3, which is an indicator of transcriptional elongation, was greatly diminished throughout the gene body of *Ephx1* in the TSS-deleted cells (Figure 1F), showing that the progression of RNA polymerase II was inhibited. In contrast, the amount of acetylated H3K27 (H3K27ac), which localizes to promoter and enhancer regions, was not substantially affected by deletion of the TSS of *Ephx1* (Figure 1G). We found that the amount of H3K27me3 was not increased in regions with a high H3K27ac level (regions f, h, and i) in the TSS-deleted cells (Figures 1E and 1G), consistent with previous results showing that acetylation and methylation of the same lysine residue compete with each other (Pasini et al., 2010).

We next examined whether a decrease in H3K27me3 level associated with transcriptional activation is reversed by CRISPR/Cas9-mediated transcriptional shutoff. For this purpose, we examined *Sorcs2*, whose transcription is driven by Ras signaling and is accompanied by removal of H3K27me3 from the gene body (Figure 2A). To delete the TSS of *Sorcs2*, we introduced a pair of sgRNAs into NIH 3T3 cells expressing a constitutively active mutant of human H-Ras (RasG12V). We established several cell clones in which the TSS of *Sorcs2* was homologously deleted (Figure 2B) and in which upregulation of *Sorcs2* expression by RasG12V was abolished, whereas expression of the Ras-regulated genes *Ephx1* and *Bpil2* was largely unaltered (Figure 2C). Ras signaling reduced the amount of H3K27me3 throughout the gene body of *Sorcs2* in parental cells, consistent with our previous observations (Hosogane et al., 2013), but this Ras-induced epigenetic alteration was abrogated by TSS deletion (Figure 2D). The Ras-induced increase in H3K36me3 abundance also was prevented by TSS deletion (Figure 2E), indicating that transcriptional elongation along the gene body of *Sorcs2* was inhibited. These observations for *Sorcs2* and *Ephx1* thus showed that H3K27me3 accumulation in the gene body was elicited by lack of transcription

(B) ChIP-seq data for H3K4me3 and RNA polymerase II (Pol II) derived from Encyclopedia of DNA Elements (ENCODE) tracks around the TSS of *Ephx1* in MEFs. Arrowheads represent the positions of sgRNAs, numbered arrows indicate primers for genotyping PCR analysis in (C), and the black bar denotes the targeted region.

(C) Genotyping PCR analysis of parental NIH 3T3 cells as well as of cells heterozygous (hetero) or homozygous (knockout) for the TSS-deleted allele of *Ephx1* generated with the CRISPR/Cas9 system is shown. WT, wild-type.

(D) RT-qPCR analysis of *Ephx1* expression in three independent *Ephx1* TSS knockout clones relative to that in parental (WT) cells is shown.

(E–G) ChIP-qPCR analysis of H3K27me3 (E), H3K36me3 (F), and H3K27ac (G) at the *Ephx1* locus in parental and *Ephx1* TSS knockout cells. Data are means ± SE for three independent clones.

See also Figure S1.

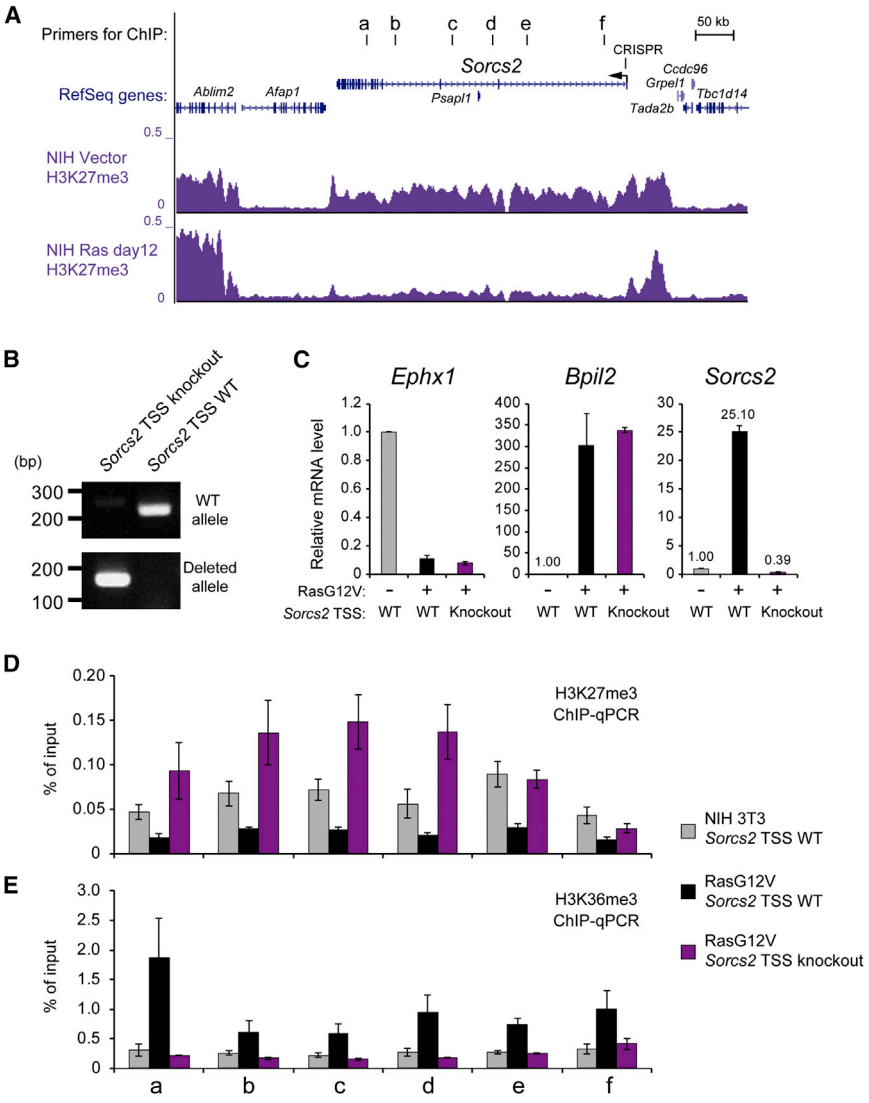

Figure 2. CRISPR/Cas9-Mediated Transcriptional Shutoff Is Sufficient to Induce Accumulation of H3K27me3 in the Gene Body of *Sorcs2*

(A) H3K27me3 level at the *Sorcs2* locus as determined by our previous ChIP-seq analysis of control NIH 3T3 cells and cells infected with a retrovirus encoding RasG12V for 12 days. The positions of ChIP-qPCR primers are indicated by lowercase letters (a–f), and the black bar represents the position of the region deleted with the CRISPR/Cas9 system. RPMs are used for the y axis in each track.

(B) Genotyping PCR analysis of parental (WT) NIH 3T3 cells as well as of cells homozygous (knockout) for the TSS-deleted allele of *Sorcs2* generated with the CRISPR/Cas9 system is shown.

(C) RT-qPCR analysis of *Ephx1*, *Bpil2*, and *Sorcs2* expression in NIH 3T3 cells expressing (or not) RasG12V with or without *Sorcs2* TSS knockout. Data are means ± SE for three independent clones.

(D and E) ChIP-qPCR analysis of H3K27me3 (D) and H3K36me3 (E) in the gene body of *Sorcs2* in parental NIH 3T3 cells and cells expressing RasG12V with or without *Sorcs2* TSS knockout. Data are means ± SE for three independent clones.

of both genes and that Ras signaling was not required for this epigenetic change.

Ras-Dependent Histone Deacetylation Induces Gene Silencing and Deposition of H3K27me3

Time course analysis revealed that the PRC2 component Suz12 was gradually recruited to the gene body as well as the region around the TSS after eviction of RNA polymerase II from *Ephx1* in response to activation of Ras signaling (Figure 3A). These data indicated that transcriptional repression is followed by PRC2 recruitment and that accumulation of H3K27me3 is not responsible for transcriptional repression by Ras signaling. We next searched for other molecular links between such signal activation and gene silencing. Acetylation of histone tails has been shown to enhance transcription, and we therefore explored the possibility that histone acetylation is controlled by the Ras-signaling pathway. To this end, we performed ChIP-qPCR analysis with antibodies to H3K27ac and to H3K27me3 at various times after the infection of NIH 3T3 cells with a retrovirus encoding RasG12V. We analyzed the genomic region around the TSS of *Ephx1* for H3K27ac and that at the 3′ end of *Ephx1* for H3K27me3. We found that the amount of H3K27ac was decreased markedly 2 days after Ras activation, at which time the amount of H3K27me3 remained unchanged (Figure 3B). Other acetylated forms of histone tails, including H3K9ac and H4ac, showed dynamics similar to those of H3K27ac in response to Ras signal activation (data not shown). These observations suggested the possibility that histone deacetylation mediates Ras-induced gene silencing, with H3K27me3 accumulating after transcriptional repression.

To test this hypothesis, we treated NIH 3T3 cells expressing RasG12V with trichostatin A (TSA), an inhibitor of histone deacetylase activity, for 5 or 6 days beginning 2 days after the activation of Ras signaling (Figure 3C). Immunoblot analysis revealed that total H3K27ac and H3K27me3 levels in NIH 3T3 cells were not affected by expression of RasG12V (Figure 3D). TSA treatment increased the total amount of H3K27ac in a concentration-dependent manner without affecting that of H3K27me3, expression of Ras, or phosphorylation (activation) of the MAPKs Erk1 and Erk2 (Figure 3D). Ras-induced deacetylation of H3K27ac in the region around the TSS of *Ephx1* was inhibited by TSA at even lower concentrations (Figure 3E). Moreover, transcription of *Ephx1* (Figure 3F) as well as recruitment of RNA polymerase II to the region around the TSS (Figure 3G) was restored by TSA treatment to levels similar to those for parental NIH 3T3 cells. Of note, the accumulation of H3K27me3 at *Ephx1* induced

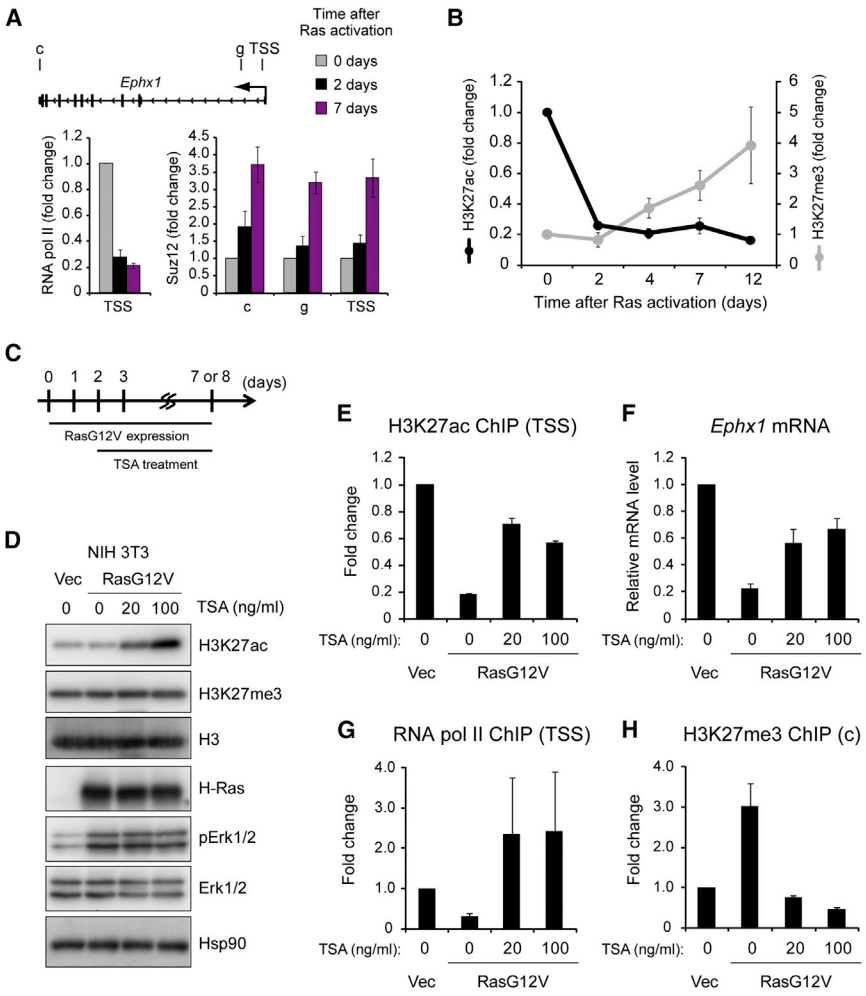

Figure 3. Histone Deacetylation Is Required for Ras-Induced Gene Silencing and Deposition of H3K27me3 at *Ephx1*

(A) ChIP-qPCR analysis of Pol II and Suz12 binding to *Ephx1* at the indicated times after infection of NIH 3T3 cells with a retrovirus encoding RasG12V. Positions of ChIP-qPCR primers for this figure are indicated in relation to *Ephx1* structure. Data are means ± SE for three independent experiments.

(B) ChIP-qPCR analysis of H3K27ac and H3K27me3 with primer sets TSS and c, respectively, at the indicated times after infection of NIH 3T3 cells with a retrovirus encoding RasG12V. Data are means ± SE for three independent experiments.

(C) Timeline for the introduction of RasG12V and exposure to TSA for NIH 3T3 cells studied in (D)–(H) is shown.

(D) Immunoblot analysis of H3K27ac, H3K27me3, total H3 (loading control), H-Ras, phosphorylated (p) and total forms of Erk1/2, and Hsp90 (loading control) in NIH 3T3 cells infected with the retrovirus encoding RasG12V (or the corresponding empty virus, Vec) and treated with the indicated concentrations of TSA is shown.

(E–H) ChIP-qPCR analysis of the effects of RasG12V and TSA both on H3K27ac level (E) and Pol II recruitment (G) in the region around the TSS of *Ephx1* and on H3K27me3 level in the gene body (H), as well as RT-qPCR analysis of *Ephx1* expression (F). Data for ChIP-qPCR are means ± SE for two independent experiments, whereas those for RT-qPCR are means ± SE for four independent experiments.

See also Figure S2.

by Ras activation was blocked by TSA (Figure 3H), suggesting that H3K27 acetylation and transcription suppress deposition of H3K27me3. Analysis of *Itgb5* yielded similar results. Ras-induced transcriptional repression and H3K27me3 deposition at *Itgb5* were thus also greatly attenuated by treatment with TSA (Figure S2). Together these observations indicated that Ras activation induces deacetylation of histone tails, which is in turn responsible for gene silencing and subsequent H3K27me3 accumulation at *Ephx1* and *Itgb5*.

Ras-Induced Accumulation of H3K27me3 Is Not Completed Until at Least 30 Days after Transcriptional Repression

Our results suggested that a change in transcriptional activity gradually influences the amount of H3K27me3 in the gene body. To determine the time required for completion of the change in H3K27me3 level induced by Ras activation, we analyzed the amount of H3K27me3 at various times up to 45 days by ChIP-qPCR analysis. Transcription of *Ephx1* was suppressed after ~5 days and remained silenced for up to 45 days (Figure 4A). By contrast, the amount of H3K27me3 along the gene body of *Ephx1* increased gradually and reached a maximum after ~35 days (Figure 4B). We also observed similar time courses of transcription and H3K27me3 accumulation for *Itgb5* (Figures S3A and S3B), suggesting that the change in H3K27me3 level for both genes takes at least 35 days to complete.

We performed ChIP-seq analysis for H3K27me3 as well as RNA sequencing (RNA-seq) analysis with the cells in which Ras signaling had been activated for 35 days. The ChIP-seq and RNA-seq results for the genomic locus containing *Ephx1* are shown together with our previous short-term time course data for H3K27me3 ChIP-seq obtained 0, 2, 4, 7, and 12 days after Ras activation (Figure 4C). In general, H3K27me3 did not manifest focal enrichment, but rather accumulated over several tens of kilobases of the genomic region. Visual inspection revealed that the amount of H3K27me3 in the gene body of *Ephx1* was much higher at 35 days than at the other time points, confirming that H3K27me3 is deposited progressively over time. To quantitate the H3K27me3 level, we used a peak caller that is optimized for detection of broad peaks. As exemplified by the *Ephx1* locus in Figure 4C, broad peaks of H3K27me3 were identified at 0 and 35 days after Ras activation. This analysis revealed that 18.7% of the entire genome was covered with

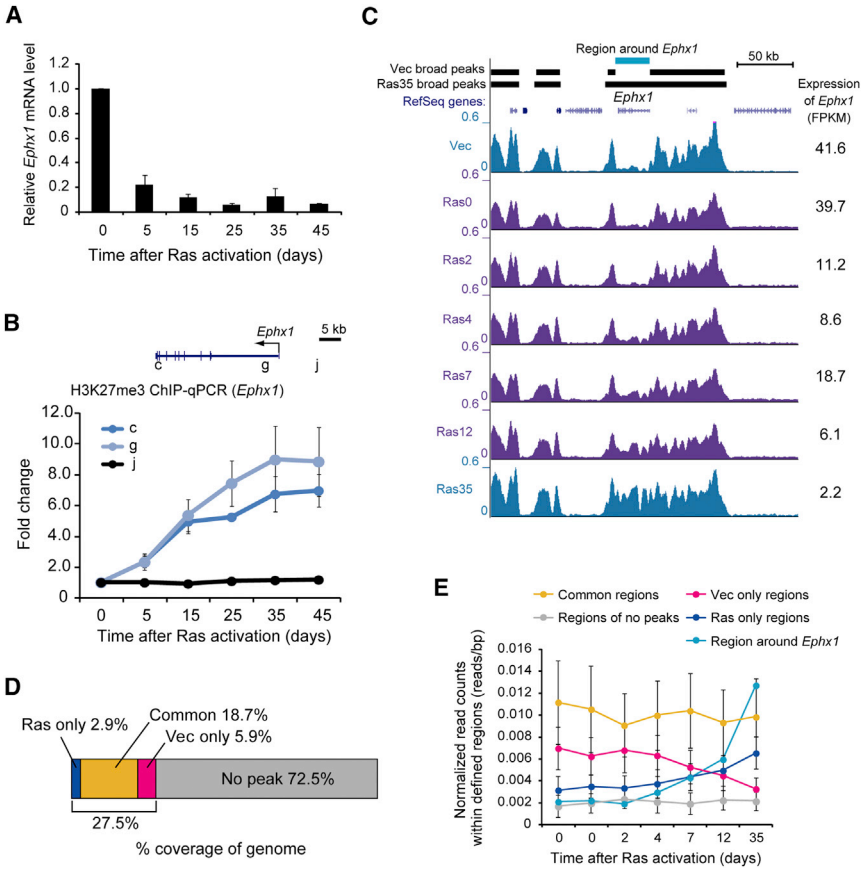

Figure 4. Accumulation of H3K27me3 at *Ephx1* Continues for at Least 35 Days after Ras Activation

(A) RT-qPCR analysis of *Ephx1* mRNA at the indicated times after introduction of RasG12V into NIH 3T3 cells. Data are means ± SE for three independent experiments.

(B) ChIP-qPCR analysis of H3K27me3 at the *Ephx1* locus at the indicated times after introduction of RasG12V into NIH 3T3 cells. The positions of primers for ChIP-qPCR are depicted at the top of the panel. Data are means ± SE for five independent experiments.

(C) Time course of changes in H3K27me3 content at the genomic region containing the *Ephx1* locus, as determined by ChIP-seq analysis of NIH 3T3 cells infected with a retrovirus for RasG12V (Ras35) or the corresponding empty virus (Vec) for 35 days. These new data are shown together with the results of our previous ChIP-seq analysis for cells at 0, 2, 4, 7, or 12 days after Ras activation. Black bars represent identified broad peaks. RPMs are used for the y axis in each track. The expression level of *Ephx1* (fragments per kilobase of exon model per million mapped reads [FPKMs]) as determined by RNA-seq analysis is shown at the right of each track.

(D) Percentage coverage of the entire genome with H3K27me3. Peaks in 2.9% and 5.9% of the genome are newly formed or lost, respectively, in response to Ras activation. Peaks identified in both control and RasG12V-expressing cells cover 18.7% of the genome, whereas no peak was identified under either condition over 72.5% of the genome.

(E) Normalized read counts for H3K27me3 ChIP-seq analysis of genomic regions (>30 kb) at the indicated times after the introduction of RasG12V into NIH 3T3 cells. The total number of H3K27me3 ChIP-seq reads was adjusted to ten million, and read counts within each region were normalized by region size (reads/base pair). Averaged values of normalized read counts for regions classified as in (D) are shown with SD values. The normalized value for the single region containing *Ephx1* also is shown.

See also Figure S3.

such broad peaks, in both control and RasG12V-expressing cells, and that 72.5% of the entire genome was devoid of such broad peaks in both types of cells (Figure 4D). Furthermore, 2.9% or 5.9% of the entire genome was not covered with H3K27me3 at day 0 but was covered at 35 days after Ras activation or vice versa.

We then calculated the normalized H3K27me3 signal within each defined H3K27me3 domain for each time point. The mean signals for both the common regions covered with H3K27me3 broad peaks and the common uncovered regions remained constant from 0 to 35 days after Ras activation (Figure 4E). In contrast, the signals for the regions covered in only control or RasG12V-expressing cells continued to change from 0 to 35 days (Figure 4E). Of note, the normalized H3K27me3 signal in the region containing *Ephx1* also showed a gradual increase (Figure 4E), with the level at 35 days being much higher than that at 12 days and similar to that for common covered regions. We obtained similar, although less pronounced, results for the genomic region containing *Itgb5* (Figure S3C). On the basis of these data, we concluded that changes in H3K27me3 content, especially around the *Ephx1* locus, were not completed until at least 35 days after Ras activation.

Transcriptional Activation with the dCas9-Activator System Erases H3K27me3 Deposited in the Gene Body of *Ephx1* in Response to Long-Term Ras Activation

To determine whether transcriptional activation is sufficient for removal of H3K27me3 broad peaks, we activated *Ephx1* transcription with the use of the dCas9-activator system based on a catalytically inactive mutant of Cas9 (dCas9) (Konermann et al., 2015). Various proteins fused to dCas9 can be recruited to specific genomic regions in the presence of sgRNAs. We first introduced RasG12V into NIH 3T3 cells and cultured the cells for at least 30 days in order to allow completion of H3K27me3 peak formation around *Ephx1*. We then sequentially introduced three components into the cells to activate *Ephx1* transcription (Figure 5A): a fusion protein consisting of dCas9 and the transcriptional activator Vp64 (dCas9-Vp64), a fusion protein containing the bacteriophage coat protein MS2 and the transactivation domains of p65 and HSF1 (MS2-p65HSF1), and a fusion RNA that includes the sgRNA and an RNA sequence with an MS2-binding site (sgRNA-MS2RNA) and mediates the recruitment of dCas9-Vp64 and MS2-p65HSF1 to the promoter region of *Ephx1* (Figure 5B).

Immunoblot analysis showed that dCas9-Vp64 was efficiently expressed without affecting the amount of Ras protein or the

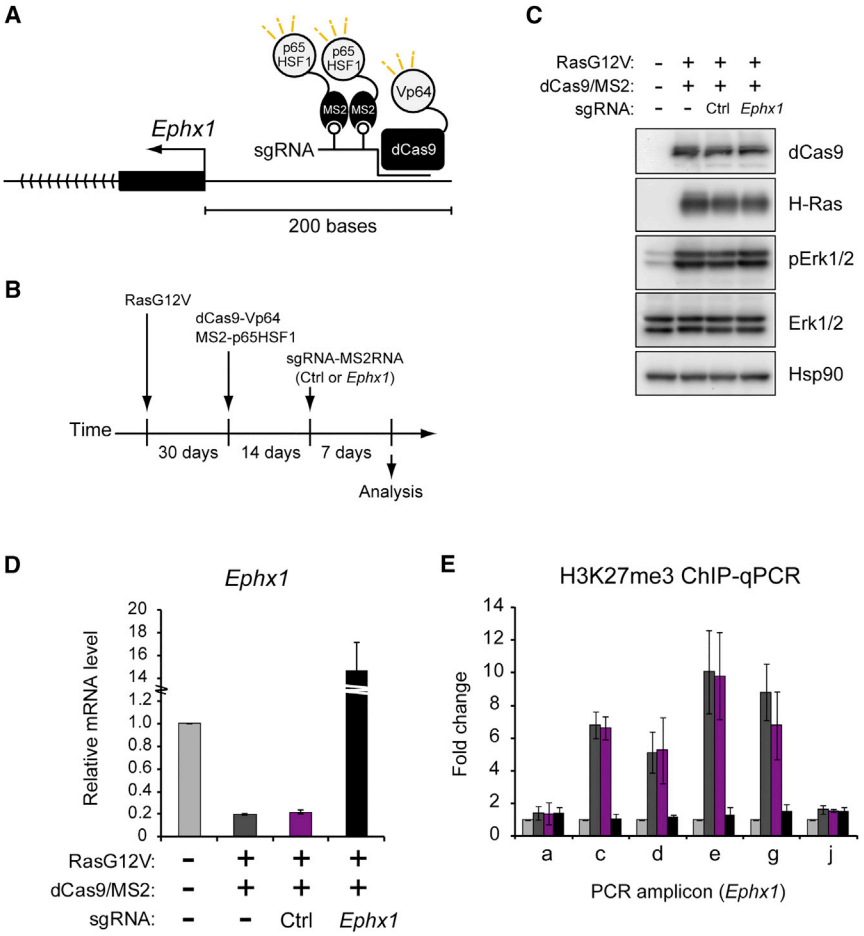

Figure 5. Transcriptional Activation Is Sufficient to Reverse H3K27me3 Accumulation at *Ephx1* Induced by Long-Term Activation of Ras Signaling

(A) Schematic representation shows the complex formed by dCas9-Vp64, MS2-p65HSF1, and sgRNA-MS2RNA in the upstream region of *Ephx1*.

(B) Timeline for experimental manipulation of *Ephx1* transcription in NIH 3T3 cells is shown. Ctrl, control.

(C) Immunoblot analysis of dCas9, H-Ras, phosphorylated (p) and total forms of Erk1/2, and Hsp90 (loading control) in NIH 3T3 cells expressing the indicated components is shown.

(D) RT-qPCR analysis of *Ephx1* expression in the manipulated cells. Data are means ± SE from two independent experiments.

(E) ChIP-qPCR analysis of H3K27me3 along the gene body of *Ephx1* in the manipulated cells. The positions of PCR amplicons are as depicted in Figure 1A. Data are means ± SE from three independent experiments.

extent of downstream-signaling activity, as indicated by the phosphorylation level of Erk1/2 (Figure 5C). Transcription of *Ephx1* was suppressed by RasG12V, and this suppression was reversed by targeting of the *Ephx1* promoter by the specific sgRNA, but it was not affected by a control sgRNA (Figure 5D). Importantly, the increase in H3K27me3 level induced by Ras signaling also was reversed by the specific sgRNA, but not by the control sgRNA (Figure 5E). Such an effect on H3K27me3 level was not observed in genomic regions external to the gene body of *Ephx1* (Figure 5E), possibly suggesting the importance of RNA polymerase II for erasure of H3K27me3. Collectively, these results showed that transcription itself erased broad peaks of H3K27me3 that had accumulated in response to prolonged activation of Ras signaling.

Effects of Forced Transcriptional Control on the Focal H3K27me3 Peak at the CpG-Rich Promoter of *Smad6*

Given that CpG islands are thought to be potential targets of PRC2 in mammalian cells (Mendenhall et al., 2010), we examined whether our results for gene bodies also might extend to H3K27me3 at CpG-rich promoters. We and others have shown that Ras signaling generates a focal H3K27me3 peak at the CpG-rich promoter of *Smad6* (Hosogane et al., 2013; Kaneda et al., 2011). In contrast to the other genes studied here, Ras induced the accumulation of H3K27me3 predominantly in the promoter region and, to a lesser extent, in the gene body of *Smad6* (Figure 6A; Figure S4A). We established several NIH 3T3 cell clones in which the TSS of *Smad6* was homologously deleted (Figure 6B). The expression level of *Smad6* in these clones was even lower than that apparent after Ras-induced gene silencing in parental cells (Figure 6C). Although Ras signaling increased the level of H3K27me3 around the CpG island in parental cells, transcriptional inhibition by TSS deletion did not trigger the focal accumulation of H3K27me3 in this region (Figure 6E). Of note, we observed an increase in H3K27me3 abundance in the gene body in response to either Ras activation or TSS deletion at sites at which the amount of H3K36me3 decreased (Figures 6D and 6E). These observations thus suggested that H3K27me3 accumulation around the CpG island of *Smad6* was not induced by abrogation of transcription alone, with Ras signaling or a DNA element within the deleted region also being required.

We also activated *Smad6* transcription with the use of the dCas9-activator system. Suppression of *Smad6* transcription by RasG12V was reversed by targeting of the gene promoter with two different specific sgRNAs (Figure S4B). Consistent with this result, the amount of H3K4me3 around the CpG island was reduced in RasG12V-expressing cells, but it was recovered in cells also expressing specific sgRNAs (Figure S4C). Importantly, the increase in H3K27me3 level induced by Ras signaling also was reversed by the specific sgRNAs, both around the CpG island as well as in the gene body of *Smad6* (Figure S4D). Collectively, these results suggested that transcriptional activation is sufficient for removal of a focal peak of H3K27me3 around a CpG island.

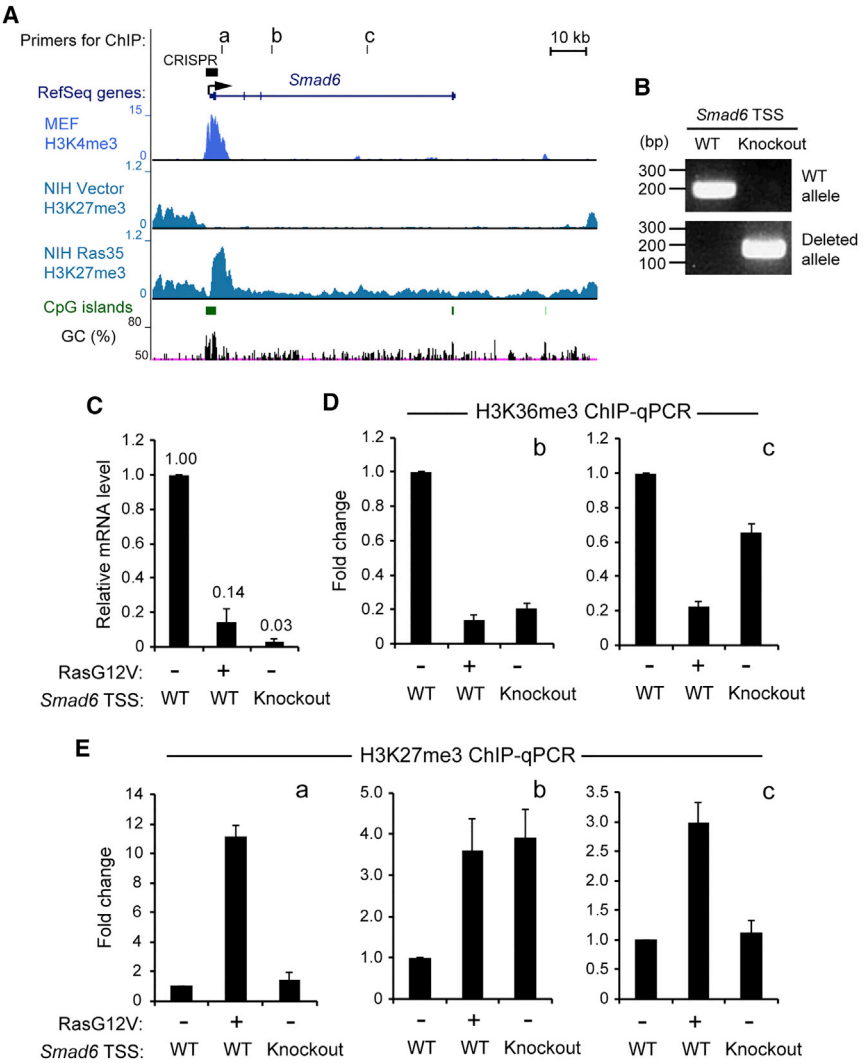

Figure 6. TSS Deletion Does Not Induce Accumulation of H3K27me3 at the CpG-Rich Promoter of *Smad6*

(A) Our ChIP-seq analysis of H3K27me3 level at the *Smad6* locus in control NIH 3T3 cells (NIH Vector) and cells at 35 days after the onset of RasG12V expression (NIH Ras35) are shown together with ChIP-seq data for H3K4me3 in MEFs, GC percentage content, and CpG islands derived from public databases. RPMs are used on the y axis for H3K27me3 ChIP-seq. The positions of ChIP-qPCR primers are indicated by the lowercase letters (a–c), and the black bar denotes the targeted region for TSS deletion.

(B) Genotyping PCR analysis of parental (WT) NIH 3T3 cells as well as of cells homozygous for the TSS-deleted allele of *Smad6* generated with the CRISPR/Cas9 system is shown.

(C) RT-qPCR analysis of *Smad6* expression in *Smad6* TSS knockout cells and RasG12V-expressing cells relative to that in parental (WT) NIH 3T3 cells. Data are means ± SE from three independent experiments (RasG12V-expressing cells) or three independent clones (TSS knockout).

(D and E) ChIP-qPCR analysis of H3K36me3 (D) and H3K27me3 (E) at the *Smad6* locus in parental, RasG12V-expressing, and *Smad6* TSS knockout cells. Data are means ± SE from three independent experiments (RasG12V-expressing cells) or three independent clones (TSS knockout).

See also Figure S4.

DISCUSSION

Although Ras signaling affects transcription and H3K27me3 level, the relation between and sequence of these events have remained unclear. We have now shown that Ras-induced changes in H3K27me3 level in the gene body are dependent on transcriptional changes. We further found that histone deacetylation is required for Ras-induced changes in both transcription and H3K27me3 level. In addition, we found that the accumulation of H3K27me3 in the gene body of *Ephx1* induced by constitutive Ras signaling required at least 35 days to reach a plateau, and we learned that even this maximal level of H3K27me3 deposition was erased by forced activation of transcription. The focal accumulation of H3K27me3 around the CpG island of *Smad6* was not induced by TSS deletion, however, although such focal deposition of H3K27me3 was erased by forced activation of transcription. Collectively, our results thus show that transcription itself regulates H3K27me3 level in the body of at least a subset of genes in cells with activated Ras signaling.

Molecular Mechanism of H3K27me3 Accumulation Induced by Transcriptional Inhibition

Chemical inhibition of RNA polymerase II with 5,6-dichloro-1-β-D-ribofuranosylbenzimidazole (DRB) or triptolide recently was shown to increase H3K27me3 abundance at CpG islands in mouse ESCs (Riising et al., 2014). This finding together with our present results indicates that certain genomic sequences have the potential to be targeted by PRC2 in the basal, untranscribed state, as has been proposed in the chromatin sampling model (Klose et al., 2013). This model suggests that RNA polymerase II itself might erase or prevent the deposition of H3K27me3 as it proceeds along the transcribed region.

At least three mechanisms have been proposed for the prevention of methyl mark deposition by RNA polymerase II: (1) given that the enzymatic activity of the PRC2 component Ezh2 is inhibited by RNA, active transcription by RNA polymerase II may maintain Ezh2 in an inactive state (Cifuentes-Rojas et al., 2014; Kaneko et al., 2013); (2) the enzymatic activity of Ezh2 is enhanced by compact chromatin where transcription is repressed (Yuan et al., 2012), and this effect would be reversed by the recruitment of RNA polymerase II; and (3) RNA polymerase II attracts H3K36 methyltransferase to the gene body via physical interaction, with H3K36me3 in turn having an inhibitory effect on PRC2 activity (Musselman et al., 2012; Schmitges et al., 2011; Yuan et al., 2011). Consistent with this

third possibility, we observed a mutually exclusive relation between H3K27me3 and H3K36me3 in cells with activated Ras signaling. Manipulation of transcription with the use of the CRISPR/Cas9 system provides direct insight into the causal nature of the relation between changes in transcription and epigenetic modification, and it represents a complementary approach for genome-wide comprehensive analysis. Further analytic substantiation is required to understand the molecular mechanisms of the chromatin sampling model as well as other possibilities.

Effects of TSS Deletion on Focal and Broad H3K27me3 Accumulation

We have shown here that the lack of transcription as a result of TSS deletion is sufficient to induce the accumulation of H3K27me3 in the gene body of *Ephx1* and *Sorcs2*. On the other hand, deletion of the TSS of *Smad6* did not induce focal accumulation of H3K27me3 in the gene promoter, but it did increase the amount of H3K27me3 in the gene body at sites at which the amount of H3K36me3 was decreased. It is thus possible that deletion of the 3.3-kb genomic region containing the TSS of *Smad6* also resulted in the loss of a DNA element responsible for the recruitment of PRC2. Given that CpG islands are thought to be potentially targeted by PRC2 in mammals, abrogation of transcription by CpG island deletion might not be sufficient to induce focal H3K27me3 accumulation. Our data are consistent with the previous observation that the inhibition of RNA polymerase II results in preferential accumulation of H3K27me3 at CpG islands (Riising et al., 2014).

Ras-Induced Histone Deacetylation Triggers Accumulation of H3K27me3

Studies of PREs in *Drosophila* have shown that PRC2 is not required for the triggering of transcriptional repression, but it is needed for maintenance of the repressed state of genes at which repression has already been established (Schwartz and Pirrotta, 2007). We also have found that initial repression was preceded by histone deacetylation, but it did not require PRC2 in the context of gene silencing dependent on Ras-MAPK signaling (Hosogane et al., 2013). Similarly, in ESCs, NuRD-mediated deacetylation of H3K27ac was found to promote PRC2 recruitment and subsequent H3K27me3 formation (Reynolds et al., 2012). Histone acetylation provides a docking site for TFIID (Filippakopoulos et al., 2012), and H3K27ac is known to compete with H3K27me3 (Pasini et al., 2010). Activation of Ras-MAPK signaling thus induces histone deacetylation, which might result in disruption of the TFIID complex at the promoter and provide substrates for PRC2.

MAPK has been found to be recruited to the TSS in order to phosphorylate serine-5 of RNA polymerase II and to regulate PRC2 in mouse ESCs (Tee et al., 2014). RNA polymerase II also is phosphorylated in response to Ras-MAPK signaling in somatic cells (Bonnet et al., 1999; Dubois et al., 1994), and we observed an increase in the abundance of the phosphorylated form of RNA polymerase II in RasG12V-expressing NIH 3T3 cells (data not shown). These data suggest that MAPK signaling might have effects on H3K27me3 levels other than that dependent on deacetylation.

Formation of Broad Peaks of H3K27me3 in Response to Transcriptional Repression

ChIP-seq analysis has revealed that H3K27me3 covers continuous genomic regions ranging from several tens to hundreds of kilobases in differentiated cells. These broad H3K27me3 domains show a cell type-specific distribution and have been designated broad local enrichments (BLOCs) (Brinkman et al., 2012; Pauler et al., 2009; Zhu et al., 2013), but the mechanism underlying their formation has remained unknown. We examined H3K27me3 accumulation in response to Ras activation to shed light on this mechanism. We found that constitutive Ras activation results in a high level of H3K27me3 accumulation from the TSS to the transcription termination site of *Ephx1*. This deposition of H3K27me3 in the gene body of *Ephx1*, together with the flanking genomic regions that are already fully decorated with this modification, gives rise to the formation of a large H3K27me3 domain similar to a BLOC. In contrast to acute changes in H3K27ac level, this change in H3K27me3 level progressed slowly and required at least 35 days for its completion. These observations suggest that H3K27me3 BLOCs in differentiated cells are established by the combination of prolonged gene silencing (in the case of the gene body) and the absence of transcription in intergenic regions.

The H3K27me3 BLOC-like domain encompassing the gene body of *Ephx1* was readily removed, however, by forced transcription with the dCas9-activator system. Moreover, we previously showed that Ras-induced H3K27me3 accumulation is insufficient to maintain the repressed state of a gene after inactivation of the Ras signal (Hosogane et al., 2013). These observations are consistent with the mutual antagonistic relation between Polycomb group proteins and transcription (Steffen and Ringrose, 2014). It remains unclear whether this antagonistic nature of H3K27me3 is related to epigenetic control of transcription in differentiated NIH 3T3 cells. Further studies are required to determine whether H3K27me3 plays a role in epigenetic memory and maintenance of the repressed state of genes in NIH 3T3 cells with activated Ras signaling, as seen in cells during differentiation in both *Drosophila* and mammals.

EXPERIMENTAL PROCEDURES

Experimental details in addition to those presented below can be found in the Supplemental Experimental Procedures.

Cells and sgRNA Design

NIH 3T3 cells were obtained from American Type Culture Collection (CRL-1658). The sgRNAs for deletion of the TSS of *Ephx1*, *Sorcs2*, or *Smad6* were designed with the use of the online CRISPR Design Tool (http://crispr.mit.edu) and were subcloned into pSpCas9(BB)-2A-Puro. The sgRNAs targeting the promoter of *Ephx1* or *Smad6* were designed with the use of the Cas9 Activator Tool (http://sam.genome-engineering.org/database) and were subcloned into lenti sgRNA(MS2)_zeo backbone. Sequences of sgRNAs are provided in the Supplemental Experimental Procedures.

Establishment of *Ephx1* TSS or *Smad6* TSS Knockout Cells and of *Sorcs2* TSS Knockout Cells Expressing RasG12V

Deletion of a genomic region containing the TSS was induced by introduction of a pair of pSpCas9(BB)-2A-Puro-based plasmids into parental NIH 3T3 cells (for *Ephx1* TSS or *Smad6* TSS deletion) or into NIH 3T3 cells expressing RasG12V (for *Sorcs2* TSS deletion) by transient electroporation with the use

of the Neon Transfection System (Life Technologies). The cells were then cloned by the limiting dilution method in 96-well plates. The resulting single cell-derived clones were screened for homozygous deletion by genomic PCR analysis with primers listed in the Supplemental Experimental Procedures.

Establishment of a Stable Cell Line Expressing dCas9-Vp64 and MS2-p65HSF1

The lenti dCAS-VP64_Blast and MS2-P65-HSF1_GFP vectors were introduced into NIH 3T3 cells expressing RasG12V by lentivirus infection. The infected cells were then subjected to selection in medium containing blasticidin (5 μg/ml), after which the GFP-positive population was sorted by flow cytometry with a BD FACS Aria2 instrument (BD Biosciences). The isolated cells, in which dCAS-VP64_Blast and MS2-P65-HSF1_GFP were stably integrated, were expanded and stored for subsequent lentivirus infection to introduce a lenti sgRNA(MS2)_zeo construct targeting the *Ephx1* or *Smad6* promoter.

Immunoblot Analysis

Immunoblot analysis was performed with antibodies to H-Ras (sc-520, Santa Cruz Biotechnology), Erk1/2 (9102, Cell Signaling Technology), phosphorylated Erk1/2 (9101, Cell Signaling Technology), Cas9 (MAC133, Millipore), Hsp90 (610418, BD Biosciences), H3K27me3 (07-449, Millipore), H3K27ac (8173, Cell Signaling Technology), and histone H3 (ab1791, Abcam).

RT-qPCR Analysis

RT-qPCR analysis was performed with primers listed in the Supplemental Experimental Procedures. Data were analyzed according to the $2^{-\Delta\Delta Ct}$ method and were normalized by the amount of *Hprt* or *Arbp* mRNA.

ChIP-qPCR Analysis

ChIP was performed with antibodies to H3K27me3 (07-449, Millipore), H3K36me3 (MABI0333, MBL), H3K27ac (8173, Cell Signaling Technology), H3K4me3 (04-745, Millipore), Suz12 (3737, Cell Signaling Technology), or RNA polymerase II (8WG16; ab817, Abcam) together with Protein A Dynabeads or Protein G Dynabeads (Life Technologies). Precipitated DNA was subjected to qPCR analysis, and data were analyzed according to the $2^{-(Ct\ of\ IP\ sample\ -\ Ct\ of\ input\ sample)}$ method and are presented as a percentage of input or fold change. Primer sequences are listed in the Supplemental Experimental Procedures.

ChIP-seq and RNA-seq

For comprehensive analysis of changes in gene expression and H3K27me3 content induced by long-term activation of Ras signaling, we performed RNA-seq and ChIP-seq analyses at 35 days after infection of NIH 3T3 cells with a retrovirus encoding RasG12V (Ras35) or with the corresponding empty virus (Vec). Figures were constructed from screen shots of the University of California, Santa Cruz (UCSC) Genome Browser with our previous time course data for H3K27me3 ChIP-seq [DNA Data Bank of Japan Sequence Read Archive, DRA: DRA001075].

ACCESSION NUMBERS

The accession number for the raw FASTQ files generated in this study is DRA: DRA004063.

SUPPLEMENTAL INFORMATION

Supplemental Information includes Supplemental Experimental Procedures and four figures and can be found with this article online at http://dx.doi.org/10.1016/j.celrep.2016.06.034.

AUTHOR CONTRIBUTIONS

M.H. and K.N. designed the study. M.H. performed the experiments, analyzed data, and wrote the paper. R.F. and M.S. organized and helped with analysis of deep sequencing. K.N. supervised the project and wrote the paper.

ACKNOWLEDGMENTS

We thank T. Kitamura for providing pMX-puro and Plat-E cells; S. Ikawa for the cDNA encoding H-Ras(G12V); T. Nagashima and Y. Nishida for help with bioinformatic analysis; Y. Nagasawa, K. Kuroda, M. Tsuda, M. Kikuchi, and M. Nakagawa for technical assistance; T. Konishi for help with preparation of the manuscript; other laboratory members for discussion; and the Biomedical Research Core of Tohoku University Graduate School of Medicine for technical support. This work was supported by grants 15K18365, 26830064, 26293059, and 15K18453 from the Japan Society for the Promotion of Science.

Received: October 12, 2015
Revised: May 7, 2016
Accepted: June 5, 2016
Published: July 7, 2016

REFERENCES

Bauer, M., Trupke, J., and Ringrose, L. (2016). The quest for mammalian Polycomb response elements: are we there yet? Chromosoma *125*, 471–496.

Blackledge, N.P., Farcas, A.M., Kondo, T., King, H.W., McGouran, J.F., Hanssen, L.L., Ito, S., Cooper, S., Kondo, K., Koseki, Y., et al. (2014). Variant PRC1 complex-dependent H2A ubiquitylation drives PRC2 recruitment and polycomb domain formation. Cell *157*, 1445–1459.

Blackledge, N.P., Rose, N.R., and Klose, R.J. (2015). Targeting Polycomb systems to regulate gene expression: modifications to a complex story. Nat. Rev. Mol. Cell Biol. *16*, 643–649.

Bonnet, F., Vigneron, M., Bensaude, O., and Dubois, M.F. (1999). Transcription-independent phosphorylation of the RNA polymerase II C-terminal domain (CTD) involves ERK kinases (MEK1/2). Nucleic Acids Res. *27*, 4399–4404.

Brinkman, A.B., Gu, H., Bartels, S.J., Zhang, Y., Matarese, F., Simmer, F., Marks, H., Bock, C., Gnirke, A., Meissner, A., and Stunnenberg, H.G. (2012). Sequential ChIP-bisulfite sequencing enables direct genome-scale investigation of chromatin and DNA methylation cross-talk. Genome Res. *22*, 1128–1138.

Cifuentes-Rojas, C., Hernandez, A.J., Sarma, K., and Lee, J.T. (2014). Regulatory interactions between RNA and polycomb repressive complex 2. Mol. Cell *55*, 171–185.

da Rocha, S.T., Boeva, V., Escamilla-Del-Arenal, M., Ancelin, K., Granier, C., Matias, N.R., Sanulli, S., Chow, J., Schulz, E., Picard, C., et al. (2014). Jarid2 Is Implicated in the Initial Xist-Induced Targeting of PRC2 to the Inactive X Chromosome. Mol. Cell *53*, 301–316.

Di Croce, L., and Helin, K. (2013). Transcriptional regulation by Polycomb group proteins. Nat. Struct. Mol. Biol. *20*, 1147–1155.

Dietrich, N., Lerdrup, M., Landt, E., Agrawal-Singh, S., Bak, M., Tommerup, N., Rappsilber, J., Södersten, E., and Hansen, K. (2012). REST-mediated recruitment of polycomb repressor complexes in mammalian cells. PLoS Genet. *8*, e1002494.

Dubois, M.F., Nguyen, V.T., Dahmus, M.E., Pagès, G., Pouysségur, J., and Bensaude, O. (1994). Enhanced phosphorylation of the C-terminal domain of RNA polymerase II upon serum stimulation of quiescent cells: possible involvement of MAP kinases. EMBO J. *13*, 4787–4797.

Dunham, I., Kundaje, A., Aldred, S.F., Collins, P.J., Davis, C.A., Doyle, F., Epstein, C.B., Frietze, S., Harrow, J., Kaul, R., et al.; ENCODE Project Consortium (2012). An integrated encyclopedia of DNA elements in the human genome. Nature *489*, 57–74.

Ernst, J., Kheradpour, P., Mikkelsen, T.S., Shoresh, N., Ward, L.D., Epstein, C.B., Zhang, X., Wang, L., Issner, R., Coyne, M., et al. (2011). Mapping and analysis of chromatin state dynamics in nine human cell types. Nature *473*, 43–49.

Erokhin, M., Elizar'ev, P., Parshikov, A., Schedl, P., Georgiev, P., and Chetverina, D. (2015). Transcriptional read-through is not sufficient to induce an

epigenetic switch in the silencing activity of Polycomb response elements. Proc. Natl. Acad. Sci. USA *112*, 14930–14935.

Filippakopoulos, P., Picaud, S., Mangos, M., Keates, T., Lambert, J.P., Barsyte-Lovejoy, D., Felletar, I., Volkmer, R., Müller, S., Pawson, T., et al. (2012). Histone recognition and large-scale structural analysis of the human bromodomain family. Cell *149*, 214–231.

Hosogane, M., Funayama, R., Nishida, Y., Nagashima, T., and Nakayama, K. (2013). Ras-induced changes in H3K27me3 occur after those in transcriptional activity. PLoS Genet. *9*, e1003698.

Kalb, R., Latwiel, S., Baymaz, H.I., Jansen, P.W., Müller, C.W., Vermeulen, M., and Müller, J. (2014). Histone H2A monoubiquitination promotes histone H3 methylation in Polycomb repression. Nat. Struct. Mol. Biol. *21*, 569–571.

Kaneda, A., Fujita, T., Anai, M., Yamamoto, S., Nagae, G., Morikawa, M., Tsuji, S., Oshima, M., Miyazono, K., and Aburatani, H. (2011). Activation of Bmp2-Smad1 signal and its regulation by coordinated alteration of H3K27 trimethylation in Ras-induced senescence. PLoS Genet. *7*, e1002359.

Kaneko, S., Son, J., Shen, S.S., Reinberg, D., and Bonasio, R. (2013). PRC2 binds active promoters and contacts nascent RNAs in embryonic stem cells. Nat. Struct. Mol. Biol. *20*, 1258–1264.

Kaneko, S., Son, J., Bonasio, R., Shen, S.S., and Reinberg, D. (2014). Nascent RNA interaction keeps PRC2 activity poised and in check. Genes Dev. *28*, 1983–1988.

Karnoub, A.E., and Weinberg, R.A. (2008). Ras oncogenes: split personalities. Nat. Rev. Mol. Cell Biol. *9*, 517–531.

Kim, K.H., and Roberts, C.W. (2016). Targeting EZH2 in cancer. Nat. Med. *22*, 128–134.

Klose, R.J., Cooper, S., Farcas, A.M., Blackledge, N.P., and Brockdorff, N. (2013). Chromatin sampling–an emerging perspective on targeting polycomb repressor proteins. PLoS Genet. *9*, e1003717.

Konermann, S., Brigham, M.D., Trevino, A.E., Joung, J., Abudayyeh, O.O., Barcena, C., Hsu, P.D., Habib, N., Gootenberg, J.S., Nishimasu, H., et al. (2015). Genome-scale transcriptional activation by an engineered CRISPR-Cas9 complex. Nature *517*, 583–588.

Mendenhall, E.M., Koche, R.P., Truong, T., Zhou, V.W., Issac, B., Chi, A.S., Ku, M., and Bernstein, B.E. (2010). GC-rich sequence elements recruit PRC2 in mammalian ES cells. PLoS Genet. *6*, e1001244.

Musselman, C.A., Avvakumov, N., Watanabe, R., Abraham, C.G., Lalonde, M.E., Hong, Z., Allen, C., Roy, S., Nuñez, J.K., Nickoloff, J., et al. (2012). Molecular basis for H3K36me3 recognition by the Tudor domain of PHF1. Nat. Struct. Mol. Biol. *19*, 1266–1272.

Pasini, D., Malatesta, M., Jung, H.R., Walfridsson, J., Willer, A., Olsson, L., Skotte, J., Wutz, A., Porse, B., Jensen, O.N., and Helin, K. (2010). Characterization of an antagonistic switch between histone H3 lysine 27 methylation and acetylation in the transcriptional regulation of Polycomb group target genes. Nucleic Acids Res. *38*, 4958–4969.

Pauler, F.M., Sloane, M.A., Huang, R., Regha, K., Koerner, M.V., Tamir, I., Sommer, A., Aszodi, A., Jenuwein, T., and Barlow, D.P. (2009). H3K27me3 forms BLOCs over silent genes and intergenic regions and specifies a histone banding pattern on a mouse autosomal chromosome. Genome Res. *19*, 221–233.

Poux, S., Horard, B., Sigrist, C.J., and Pirrotta, V. (2002). The Drosophila trithorax protein is a coactivator required to prevent re-establishment of polycomb silencing. Development *129*, 2483–2493.

Ran, F.A., Hsu, P.D., Wright, J., Agarwala, V., Scott, D.A., and Zhang, F. (2013). Genome engineering using the CRISPR-Cas9 system. Nat. Protoc. *8*, 2281–2308.

Reynolds, N., Salmon-Divon, M., Dvinge, H., Hynes-Allen, A., Balasooriya, G., Leaford, D., Behrens, A., Bertone, P., and Hendrich, B. (2012). NuRD-mediated deacetylation of H3K27 facilitates recruitment of Polycomb Repressive Complex 2 to direct gene repression. EMBO J. *31*, 593–605.

Riising, E.M., Comet, I., Leblanc, B., Wu, X., Johansen, J.V., and Helin, K. (2014). Gene silencing triggers polycomb repressive complex 2 recruitment to CpG islands genome wide. Mol. Cell *55*, 347–360.

Sarma, K., Cifuentes-Rojas, C., Ergun, A., Del Rosario, A., Jeon, Y., White, F., Sadreyev, R., and Lee, J.T. (2014). ATRX directs binding of PRC2 to Xist RNA and Polycomb targets. Cell *159*, 869–883.

Schmitges, F.W., Prusty, A.B., Faty, M., Stützer, A., Lingaraju, G.M., Aiwazian, J., Sack, R., Hess, D., Li, L., Zhou, S., et al. (2011). Histone methylation by PRC2 is inhibited by active chromatin marks. Mol. Cell *42*, 330–341.

Schmitt, S., Prestel, M., and Paro, R. (2005). Intergenic transcription through a polycomb group response element counteracts silencing. Genes Dev. *19*, 697–708.

Schwartz, Y.B., and Pirrotta, V. (2007). Polycomb silencing mechanisms and the management of genomic programmes. Nat. Rev. Genet. *8*, 9–22.

Simon, J.A., and Kingston, R.E. (2013). Occupying chromatin: Polycomb mechanisms for getting to genomic targets, stopping transcriptional traffic, and staying put. Mol. Cell *49*, 808–824.

Steffen, P.A., and Ringrose, L. (2014). What are memories made of? How Polycomb and Trithorax proteins mediate epigenetic memory. Nat. Rev. Mol. Cell Biol. *15*, 340–356.

Surface, L.E., Thornton, S.R., and Boyer, L.A. (2010). Polycomb group proteins set the stage for early lineage commitment. Cell Stem Cell *7*, 288–298.

Tee, W.W., Shen, S.S., Oksuz, O., Narendra, V., and Reinberg, D. (2014). Erk1/2 activity promotes chromatin features and RNAPII phosphorylation at developmental promoters in mouse ESCs. Cell *156*, 678–690.

Yuan, W., Xu, M., Huang, C., Liu, N., Chen, S., and Zhu, B. (2011). H3K36 methylation antagonizes PRC2-mediated H3K27 methylation. J. Biol. Chem. *286*, 7983–7989.

Yuan, W., Wu, T., Fu, H., Dai, C., Wu, H., Liu, N., Li, X., Xu, M., Zhang, Z., Niu, T., et al. (2012). Dense chromatin activates Polycomb repressive complex 2 to regulate H3 lysine 27 methylation. Science *337*, 971–975.

Zheng, Q., Cai, X., Tan, M.H., Schaffert, S., Arnold, C.P., Gong, X., Chen, C.Z., and Huang, S. (2014). Precise gene deletion and replacement using the CRISPR/Cas9 system in human cells. Biotechniques *57*, 115–124.

Zhu, J., Adli, M., Zou, J.Y., Verstappen, G., Coyne, M., Zhang, X., Durham, T., Miri, M., Deshpande, V., De Jager, P.L., et al. (2013). Genome-wide chromatin state transitions associated with developmental and environmental cues. Cell *152*, 642–654.